# Nonlinear Viscoelastic Dynamics of Nanoconfined Wetting Liquids

Tai-De Li and Elisa Riedo

*School of Physics, Georgia Institute of Technology, Atlanta, Georgia 30332, USA*
(Received 9 May 2007; revised manuscript received 24 September 2007; published 13 March 2008)

The viscoelastic dynamics of nanoconfined wetting liquids is studied by means of atomic force microscopy. We observe a nonlinear viscoelastic behavior remarkably similar to that widely observed in metastable complex fluids. We show that the origin of the measured nonlinear viscoelasticity in nanoconfined water and silicon oil is a strain rate dependent relaxation time and slow dynamics. By measuring the viscoelastic modulus at different frequencies and strains, we find that the intrinsic relaxation time of nanoconfined water is in the range 0.1–0.0001 s, orders of magnitude longer than that of bulk water, and comparable to the dielectric relaxation time measured in supercooled water at 170–210 K.

Confined fluids exhibit unique structural, dynamical, electrokinetic, and mechanical properties that are different from those of the bulk [1–9]. Their behavior depends on the degree of confinement, strain rate, temperature, fluid molecular structure, and interactions with boundaries. Surprising effects have been found when water is confined in nanogaps:, for example, the electric field induced freezing of water at room temperature [10] and the extremely high viscosity of water close to a mica surface [1,4,11]. Previous experiments and calculations have pointed out the key role of the confining surfaces [1,6]. A notable increase in viscosity and decrease in the diffusion constant was measured only when water was confined between hydrophilic surfaces. For hydrophobic confinement, the observed increase of viscosity was not very pronounced. Intriguingly, a similar behavior has been observed in confined glassy materials. When a glass-forming fluid is cooled down to the glass transition temperature $T_g$, its viscosity grows by many orders of magnitude, and the confinement can increase or decrease $T_g$ for strong or weak interactions with the walls, respectively [9].

So far, the viscosity measurements for nanoconfined water have been performed in the linear viscoelastic regime. However, as observed in *macroscopic* rheological measurements, the study of the viscoelastic properties as a function of shear amplitude and rate is important for a better understanding of the dynamical and structural properties of fluids [12].

In this Letter, we investigate the viscoelastic response of nanoconfined water and silicon oil (octamethylcylotetrasiloxane, OMCTS), as a function of shear amplitude and rate, by means of direct high-resolution atomic force microscopy (AFM) measurements. We observe a nonlinear viscoelastic behavior remarkably similar to that widely observed in metastable complex fluids, such as gels and supercooled liquids [12–14]. The origin of this nonlinear viscoelasticity in nanoconfined water and in other nanoconfined wetting liquids is a strain rate dependent relaxation time and slow dynamics. By measuring the visco-

elastic modulus at different frequencies and strains, we find that the intrinsic relaxation time $\tau_0$ of nanoconfined water is in the range 0.1–0.0001 s, orders of magnitude longer than that of bulk water, and comparable to the dielectric relaxation time measured in supercooled water at 170–210 K [15].

In our AFM experiments [1,2], a nanosize spherical silicon tip is brought quasistatically to the vicinity of a flat freshly tape-cleaved hydrophilic mica surface, all immersed in purified water or OMCTS, while small lateral oscillations are applied to the cantilever support [1]. The normal and lateral forces acting on the tip are measured directly and simultaneously as a function of the liquid film thickness, i.e., tip-sample distance $d$. The zero distance $d = 0$ is evaluated by comparison of the normal force vs $d$ curves with contact mechanics models [1].

The experiments were performed with a Molecular Imaging PicoPlus AFM. We used silicon tips with radii $R = 40 \pm 10$ nm and Ultrasharp NSC12/50 cantilevers with normal and lateral spring constant in the range $k_N = 3–4.5$ N/m and $k_L = 50–120$ N/m, respectively. In our experiments, the AFM tips apex is spherical, but might not be atomically smooth; however, the viscoelastic behavior was found to be reproducible for different tips. The calibration and force detection was performed as described in Refs. [1,2]. The approach velocity was 0.2 nm/s. During the approach, lateral oscillations parallel to the mica surface were applied to the cantilever holder by means of a lock-in amplifier. The same lock-in amplifier was then used to measure the amplitude of the lateral force $F_L$ and the phase difference $\theta$ between the applied lateral displacement and the detected lateral force. The $\theta = 0$ was chosen when the tip was in hard contact with the mica surface, for lateral oscillation amplitudes $X_0$, small enough to guarantee an elastic contact without slippage [16]. In order to insure that the shear is perfectly parallel to the mica surface we have followed the procedure described in Ref. [1]. All the experiments were performed at 300 K in high purity DIUF water ($p$H = 6.1) or OMCTS. The purity of water

used in our AFM liquid cell was tested before and after the
experiments as described in Refs. [1,17].

When a viscoelastic material is confined between two
parallel plates separated by $d$, with area $A$, and a sinusoidal
strain is applied to one of the plates at the frequency $\omega$,
$\gamma = \gamma_0 \sin(\omega t)$, the resulting stress between the plates can
be written as $\sigma = \sigma_0 \sin(\omega t + \theta)$. The relationship be-
tween the strain amplitude $\gamma_0 = \frac{X_0}{d}$ and the stress ampli-
tude $\sigma_0 = \frac{F_L}{A}$ is given by

$$\frac{F_L}{A} = |G^*| \frac{X_0}{d}, \qquad (1)$$

where $G^*$ is the viscoelastic modulus. The viscoelastic
modulus contains the dissipative and elastic response of
the confined material. In particular, $G^*$ can be written as a
complex sum of the storage modulus $G'$ and the loss
modulus $G''$, i.e., $G^* = G' + iG''$, where [18]:

$$G' = \frac{F_L d}{A X_0} \cos\theta, \qquad G'' = \frac{F_L d}{A X_0} \sin\theta. \qquad (2)$$

For a purely elastic solid, $\sigma$ and $\gamma$ remain in phase, $\theta = 0$,
and so $G'' = 0$ and $G' = G^*$.

In order to study the viscoelastic behavior of nanocon-
fined water we have measured $F_L$ and $\theta$ when we laterally
oscillate the AFM cantilever holder. As a first approxima-
tion, the lateral spring constant of our silicon cantilever is
much larger than the lateral tip-water contact stiffness for
$d < 1$ nm [19]. As a consequence, the applied oscillation
amplitude to the cantilever holder is equal to the shear
amplitude of the tip apex. Figure 1 shows $F_L$ and $\theta$ as a
function of $d$ for three different shear amplitudes at $\omega =$

955.3 Hz. For tip-sample distances larger than 1 nm, $F_L$ is
equal to zero within the instrumental error for any $X_0$. As
soon as $d < 1$ nm, $F_L$ increases with decreasing $d$, and
almost diverges at $d = 0$ nm when the tip is in hard contact
with the mica surface. In a previous study [1], $F_L$ has been
used to calculate the viscosity of water ($\eta$) by using
Eq. (1), and by considering water as purely viscous, that
is, by making the approximation $|G^*| \approx G'' \approx \eta\omega$. This
approximation is true when $\theta \cong 90°$, which, as we show
later, is the case for large strain rate amplitudes defined as
$\dot{\gamma}_0 \equiv \gamma_0\omega$. However, the phase measurements presented in
Fig. 1 show that in general the behavior of nanoconfined
water is viscoelastic, and furthermore, $F_L$ does not grow
proportionally with the shear amplitude, nor with $\omega$ (not
shown here). This indicates that the viscoelastic response is
not linear, and the viscoelastic modulus is shear amplitude
dependent, $G^* = G^*(\gamma_0)$. Therefore, a detailed study of $G^*$
as a function of $\gamma_0$ is needed to shed light into this non-
linear behavior.

By applying Eq. (2) to the data in Fig. 1, we have
extracted $G'$ and $G''$ as a function of $d$ for different $X_0$ at
a fixed $\omega$. [The $A$ used for Eq. (2) is the contact area
corresponding to the spherical segment defined by the
intersection between the spherical tip and a plane at $z =
d + \triangle h$, $\Delta h = 0.25$ nm, i.e., a water molecule diameter
[1].] Figure 2 shows very clearly that $G'$ and $G''$ strongly
depend on $X_0$. For large $X_0$, $G''$ dominates over $G'$, the
response of nanoconfined water becomes purely viscous.
Also, by decreasing the gap size, the rise of $G'$ and $G''$
takes place *later* (smaller $d$) for larger $X_0$. Furthermore, for
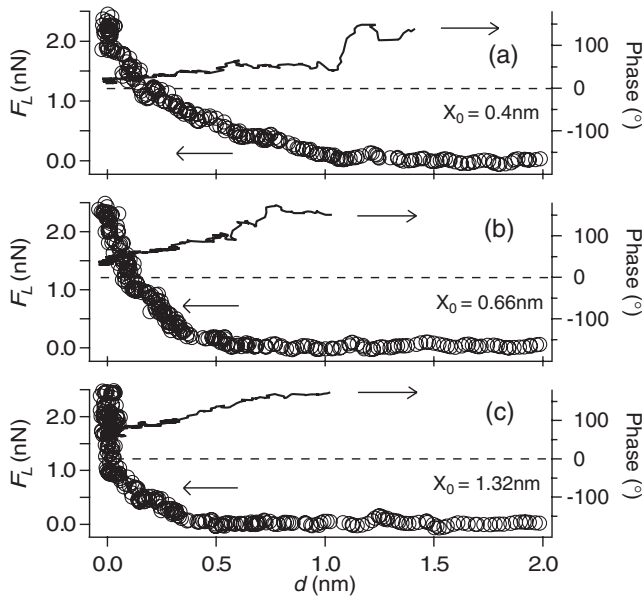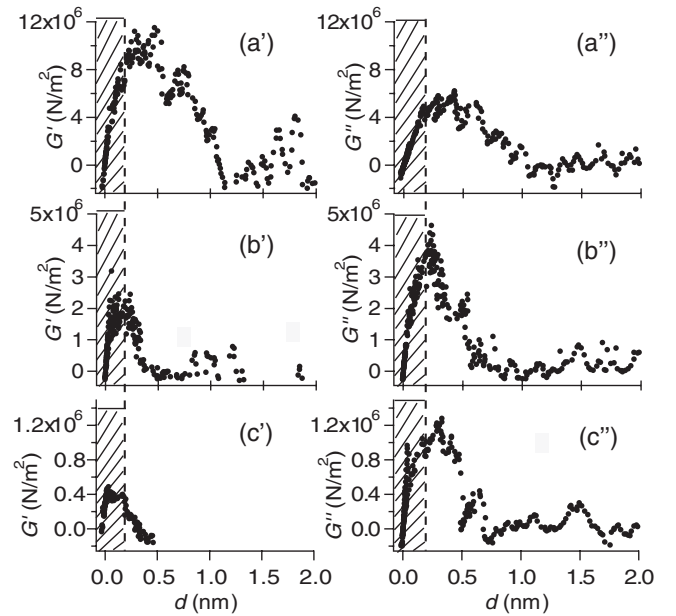


FIG. 1.   $F_L$ and $\omega$ in water as a function of $d$ at $\omega = 955.3$ Hz,
and for three different $X_0$ values, (a) $X_0 = 0.4$ nm. (b) $X_0 =
0.66$ nm. (c) $X_0 = 1.32$ nm. The phase for $d > 1$ nm is not
shown because it fluctuates randomly.



FIG. 2.   $G'$ and $G''$ in water as a function of tip-sample dis-
tance. The shadowed area, $d < 0.2$ nm, is not discussed in this
Letter because the gap size is smaller than a water molecular
dimension. $\omega$ is 955.3 Hz, and the $X_0$ is 0.4 nm for (a') and (a''),
0.66 nm for (b') and (b''), and 1.32 nm for (c') and (c'').

all the investigated $X_0$, the rise of $G''$ occurs *earlier* (larger $d$) than the rise of $G'$. The dramatic drop of both $G'$ and $G''$ for $d < 0.2$ nm (shadowed area in Fig. 2) is due to the invalidity of Eq. (2) for $d$ smaller than the dimension of one water molecule. Figure 2 indicates that the shear amplitude dependence of the viscoelastic modulus is very complex and nonlinear. For this reason we have performed measurements over a large range of $X_0$ and $\omega$ (0.06 nm $< X_0 <$ 2.8 nm, 50 Hz $< \omega <$ 2 kHz).

Following the Maxwell model for a linear viscoelastic system, the relationship between the intrinsic relaxation time $\tau_0$ and the moduli, $G'$ and $G''$, is given by [18]

$$G' = \frac{G_0(\omega\tau_0)^2}{1 + (\omega\tau_0)^2}, \qquad G'' = \frac{G_0(\omega\tau_0)}{1 + (\omega\tau_0)^2}, \qquad (3)$$

where $G_0$ is a constant. According to Eq. (3), $G'$ and $G''$ do not depend explicitly on $\gamma_0$. However, many metastable complex fluids experience a drastic decrease of their structural relaxation time when they are subjected to large strains. This phenomenon gives rise to a strong strain dependence of $G'$ and $G''$, which can be described by the introduction of an *effective* relaxation time $\tau$ that depends on the *intrinsic* relaxation time and the strain rate, $\dot{\gamma}_0 = \gamma_0\omega$ [12]. Once defined $\tau$, it is used to replace $\tau_0$ in Eq. (3), and thus to predict $G'$ and $G''$ as a function of the strain. Recently, a phenomenological expression has been found to characterize a $\dot{\gamma}_0$ dependent effective relaxation time in metastable complex fluids [12]

$$\frac{1}{\tau} \simeq \frac{1}{\tau_0} + K \cdot \dot{\gamma}_0^{\nu}, \qquad (4)$$

where $\nu$ is a positive exponent, and $K$ is a constant. In a glassy system which shows slow dynamics ($\omega \gg \frac{1}{\tau_0}$), $\nu \sim 1$ and $K \sim 1$ [20]. By replacing $\tau_0$ in Eq. (3) with $\tau$ in Eq. (4) when $\omega \gg \frac{1}{\tau_0}$, the maximum of $G''$ is near $\gamma_0 \simeq 1$, independently of the $\omega$. Figure 3 presents $G'$ and $G''$ vs $\gamma_0$ for nanoconfined water, obtained by applying Eq. (2) to the measured $F_L$ and $\theta$ at three different $\omega$ for $d = 0.4$ nm. In Fig. 3, $G'$ and $G''$ show remarkable behavior: (i) the peak position of $G''$ is around $\gamma_0 \simeq 1$ over a wide range of frequencies; (ii) for $\gamma_0 < 1$, the viscoelasticity is dominantly elastic, i.e., $G' > G''$; and (iii) $G'$ and $G''$ decay to zero for large values of $\gamma_0$. These features of our nanoconfined water system are ubiquitous in metastable complex fluids [12] and they are all captured by the argument of the strain rate dependent $\tau$. Indeed, by using Eqs. (3) and (4) the shape of the curves presented in Fig. 3 can be fully described. In order to understand if other fluids, Newtonian in the nonconfined state, behave like metastable complex fluids and follow Eqs. (3) and (4) once confined, we performed the same measurements in nanoconfined OMCTS. OMCTS is a mica-wetting nonpolar liquid, with a molecular diameter of about 0.7 nm. From the measurements shown in the insets of Figs. 3 and 4, it is clear that, also nanoconfined OMCTS presents a nonlinear
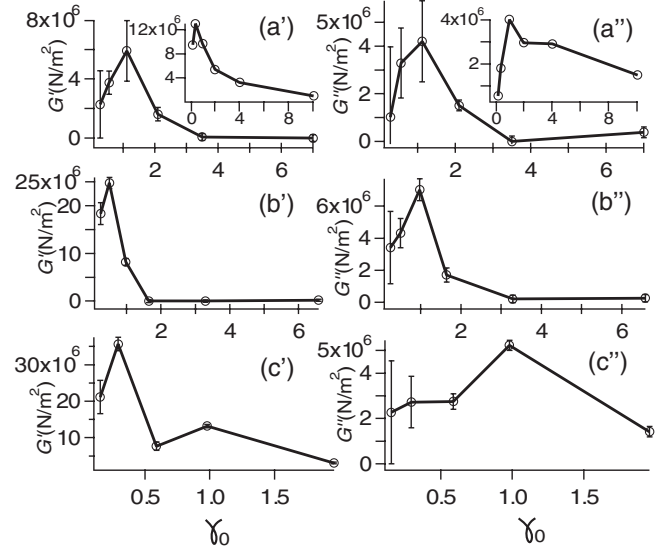


FIG. 3.   At $d = 0.4$ nm, $G'$ and $G''$ in water as a function of $\gamma_0 = X_0/d$, and $\omega$ is 52.02 Hz for (a') and (a''), 955.3 Hz for (b') and (b''), and 1.9689 kHz for (c') and (c''). The insets show the results for OMCTS at $d = 1.4$ nm.

viscoelasticity with strain rate dependent effective relaxation times.

From Eq. (3), $\tau$ can be predicted by

$$\tau = \frac{G'}{G''} \cdot \frac{1}{\omega}. \qquad (5)$$

By using Eq. (5) and the experimental values of $G'$ and $G''$, $\tau$ as a function of $\dot{\gamma}_0$ for water at $d = 0.4$ nm is determined and shown in Fig. 4. The effective relaxation time of nanoconfined water decreases from 40 to 0.7 ms when $\dot{\gamma}_0$ increases from 14 to 6000 s$^{-1}$. The nonlinearity of the relaxation time sets in when the experimental time scale ($\dot{\gamma}_0$) is faster than the intrinsic relaxation time ($\tau_0$). In this case, the time response can only be measured effectively as a function of the experimental time scale.
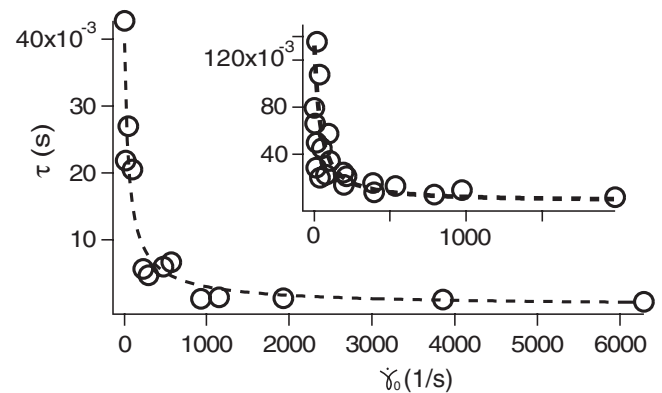


FIG. 4.   $\tau$ vs $\dot{\gamma}_0$ for water at $d = 0.4$ nm. The dashed line is the fitting with Eq. (4) for $K = 0.95 \pm 1.49$ and $\nu = 0.84 \pm 0.29$ [20]. In the inset, the results are shown for OMCTS at $d = 1.4$ nm.

By fitting the data in Fig. 4 with Eq. (4) we found that $\tau_0 = 0.06 \pm 0.03$ s for nanoconfined water at $d = 0.4$ nm. In OMCTS, $\tau_0$ is longer than in water for the same $d$, in particular, $\tau_0 \sim 0.13$ s for $d = 1.4$ nm. The striking result is that the observed $\tau$ and $\tau_0$ are orders of magnitude slower than the relaxation time of bulk water and OMCTS at room temperature. The fact that confinement can drastically slow down the dynamics of a fluid has been previously observed in diverse systems [21], such as colloidal suspensions [22], and polymers [7], where for strong fluid-wall interactions, the glass transition temperature is shifted towards high temperatures upon confinement [9]. An alternative way to view this behavior is to consider that the confinement defines an effective temperature of the system which is lower than the canonical temperature [23]. According to a previous study [15], the dielectric relaxation time of supercooled water confined in clays at 175 K is about 0.06 s, similar to the relaxation time found in our experiments on nanoconfined water at room temperature. Moreover, the value of the viscosity measured in our investigations is comparable with that of supercooled water at 140 K in a 100 $\mu$m radius tube [24]. A recent study has shown that the dielectric relaxation time of supercooled water is very sensitive to the confinement [25]. For confinement lengths of the order of 1 nm, it was found that, over a wide range of temperatures, the dielectric relaxation times are always longer than in bulk water. In our experiments, we also observe that $\tau$ is longer for increased confinement, i.e., with decreasing $d$. Unfortunately, for $d \gtrsim 1$ nm $F_L$ becomes too small to measure precisely due to low signal-to-noise ratio. The only information that we can extract is that the intrinsic relaxation time for $d \gtrsim 1$ nm is shorter than $10^{-4}$ s.

In conclusion, we have studied the viscoelastic properties of nanoconfined wetting liquids at 300 K, finding a slow dynamical behavior similar to that observed in metastable complex fluids. By measuring the viscoelastic modulus at different frequencies and strains, we find that the intrinsic relaxation time of nanoconfined water is $\approx 0.06$ s. This value is comparable with the dielectric relaxation time measured in supercooled water at 175 K.

[1] T.-D. Li, J. Gao, R. Szoszkiewicz, U. Landman, and E. Riedo, Phys. Rev. B **75**, 115415 (2007).

[2] R. Szoszkiewicz and E. Riedo, Phys. Rev. Lett. **95**, 135502 (2005).

[3] E. Riedo, F. Levy, and H. Brune, Phys. Rev. Lett. **88**, 185505 (2002).

[4] M. Antognozzi *et al.*, Appl. Phys. Lett. **78**, 300 (2001).

[5] S. Jeffery *et al.*, Phys. Rev. B **70**, 054114 (2004).

[6] T. Uchihashi *et al.*, Nanotechnology **16**, S49 (2005).

[7] M. Alcoutlabi and G. B. McKenna, J. Phys. Condens. Matter **17**, R451 (2005).

[8] R. C. Major *et al.*, Phys. Rev. Lett. **96**, 177803 (2006).

[9] P. Scheidler *et al.*, Europhys. Lett. **59**, 701 (2002).

[10] E.-M. Choi *et al.*, Phys. Rev. Lett. **95**, 085701 (2005).

[11] Y. Zhu and S. Granick, Phys. Rev. Lett. **87**, 096104 (2001).

[12] K. Miyazaki *et al.*, Europhys. Lett. **75**, 915 (2006).

[13] M. D. Ediger *et al.*, J. Phys. Chem. **100**, 13200 (1996).

[14] N. Giovambattista *et al.*, J. Phys. Chem. B **108**, 6655 (2004).

[15] S. Cerveny *et al.*, Phys. Rev. Lett. **93**, 245702 (2004).

[16] R. W. Carpick *et al.*, Appl. Phys. Lett. **70**, 1548 (1997).

[17] We performed contact angle ($\theta_c$) measurements on a (i) freshly cleaved mica surface, (ii) mica surface where we left to evaporate all the water used in our experiment, and (iii) mica surface where the water used in the experiments is gently poured out of the liquid cell. The first and third measurements give the same $\theta_c$, while in the second measurement $\theta_c$ increases. These results suggest that the impurities in our water are not surface active. We also performed conductivity measurements indicating a concentration of impurities equal to $1.3 \times 10^{-5}$ mole/l. By considering that the volume of interest is defined by the confined space between the AFM tip and the mica surface, i.e., about 120 nm$^3$ for $d = 2$ nm, we estimate that in the confined region there are $10^{-3}$ impurity molecules. Finally, before and after each measurement, we take AFM topography and friction images of the mica surface to avoid any contaminated and/or inhomogeneous area.

[18] J. D. Ferry, *Viscoelastic Properties of Polymers* (Wiley, New York, 1980), 3rd ed.

[19] From the results in Fig. 2, the shear elastic modulus of nanoconfined water $G'$ is 3 orders of magnitude smaller than the shear modulus of silicon, $G^s \simeq 50$ GPa. The tip-water contact lateral stiffness is approximately equal to $K_L^c \sim 8a(\frac{1}{G'} + \frac{1}{G^s})^{-1} \sim 0.4$ N/m ($a$ is the contact radius, $a \simeq 4.5$ nm in these experiments), which is 2 orders of magnitude smaller than the torsion and lateral force constant.

[20] K. Miyazaki and D. R. Reichman, Phys. Rev. E **66**, 050501(R) (2002).

[21] H.-W. Hu *et al.*, Phys. Rev. Lett. **66**, 2758 (1991).

[22] C. R. Nugent *et al.*, Phys. Rev. Lett. **99**, 025702 (2007).

[23] M.-C. Bellissent-Funel, J. Phys. Condens. Matter **13**, 9165 (2001).

[24] J. Hallett, Proc. Phys. Soc. London **82**, 1046 (1963).

[25] J. Swenson *et al.*, Phys. Rev. Lett. **96**, 247802 (2006).